Cell Reports, Volume *7*

Supplemental Information

APP Homodimers Transduce an Amyloid-β-Mediated Increase in Release Probability at Excitatory Synapses

Hilla Fogel, Samuel Frere, Oshik Segev, Shashank Bharill, Ilana Shapira, Neta Gazit, Tiernan O'Malley, Edden Slomowitz, Yevgeny Berdichevsky, Dominic M. Walsh, Ehud Y. Isacoff, Joel A. Hirsch, and Inna Slutsky

Supplemental Figures

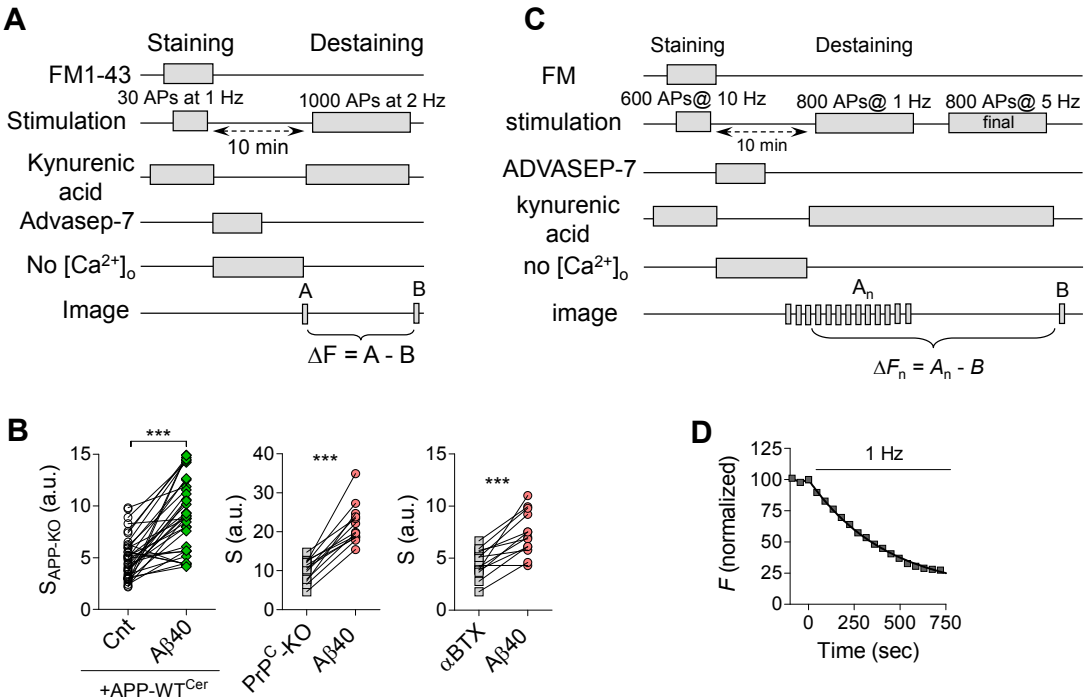

Figure S1, related to Figure 1. Determining effect of Aβ on probability of synaptic vesicle release

(A) Experimental protocol used for analysis of synaptic vesicle recycling by FM staining.

(B) *Left*: Transfection of APP$^{-/-}$ neurons with APP-WT tagged to Cerulean rescued the effect of Aβ (100 pM) on synaptic vesicle recycling (n = 38, N = 8, 2.1-fold increase, p < 0.0001). *Middle*: Aβ40 (100 pM) increases synaptic vesicle recycling in PrP^{C}-KO hippocampal neurons (n = 13, p < 0.0001). *Right*: Aβ40

(100 pM) increases synaptic vesicle recycling in wild-type neurons pretreated by 100 nM αBTX (n = 13, p < 0.0001).

(C) Experimental protocol used for analysis of synaptic vesicle release by FM destaining rate.

(D) Representative data demonstrating FM4-64 destining rate constant during 1 Hz stimulation (*k*).

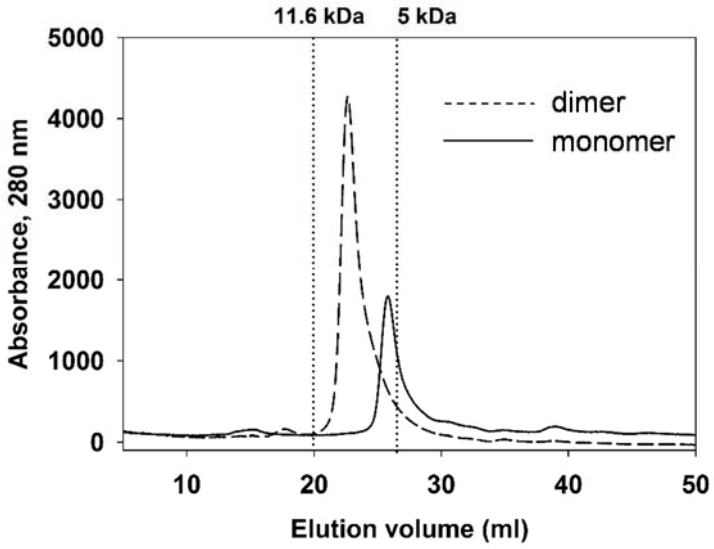

Figure S2, related to Figure 1. Determination of Aβ40 oligomeric state. Analytical SEC elution profiles of monomeric (solid line) and dimeric (dash line) Aβ40S26C using superdex 75, 10/300 GL column. Samples (100 μl of 50 μM) were injected and compared to the elution profiles of unbranched dextran with molecular weight of 5 kDa and 11.5 kDa, represented by vertical dotted lines.

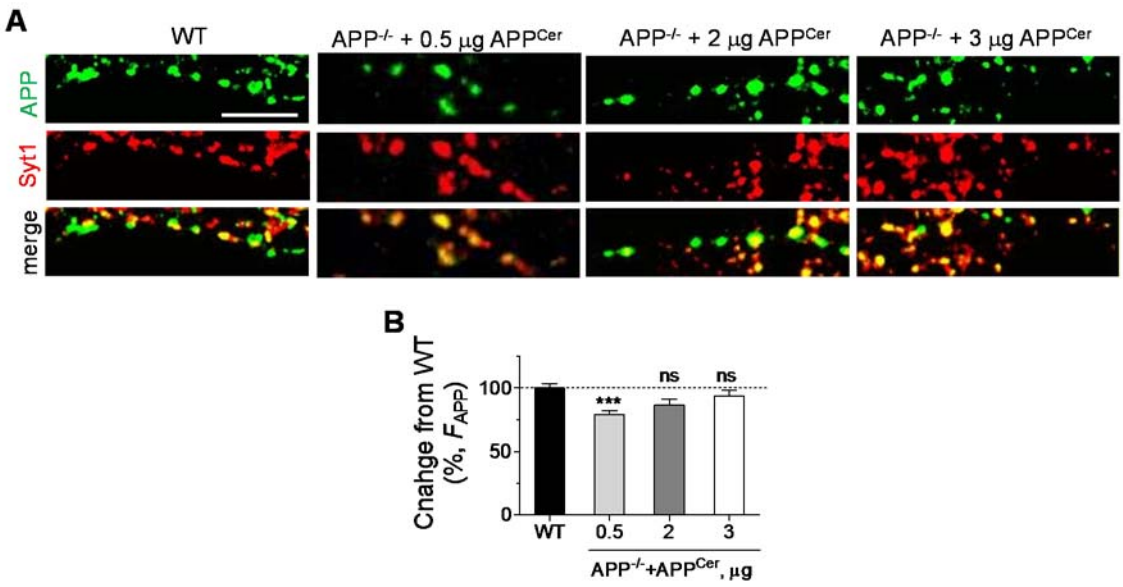

Figure S3, related to Figure 2. Quantification of APP expression at presynaptic sites in WT versus *APP*$^{-/-}$ hippocampal cultures transfected with APP^{Cer}

(A) Combined immunofluorescence detection of APP (green, using Y188 antibody) and synaptophysin-1 (Syt1, red) in WT cultured hippocampal neurons versus APP$^{-/-}$ transfected with different amount of APP^{Cer} (0.5, 2 and 3 ug; empty vector was added to preserve the total amount of cDNA constant). Scale bar: 5 μm. Colocalized APP/Syt1 puncta were detected in superimposed APP and Syt1 images (merge).

(B) Fluorescence intensity of APP in Synaptophysin-1 positive puncta (n = 96, 84, 43 and 83 in WT, APP$^{-/-}$ expressing 0.5, 2 and 3 μg of APP^{Cer}, respectively). Transfection with 2 or 3 ug of APP^{Cer} cDNA resulted in the level of presynaptic APP^{Cer} expression which was similar to those of endogenous APP in WT neurons ($p > 0.05$, one-way ANOVA).

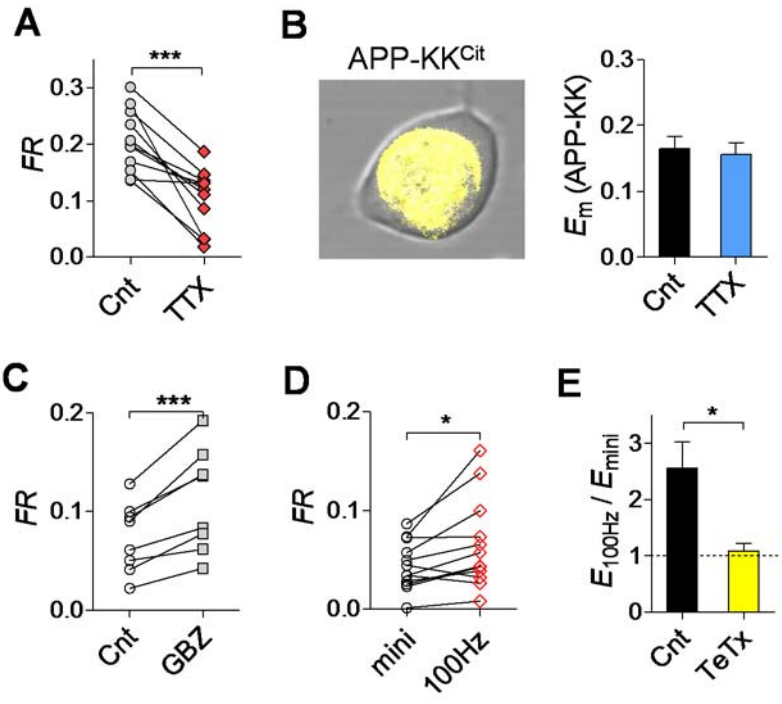

Figure S4, related to Figure 2. Monitoring activity-dependent changes in APP^{Cit}-APP^{Cer} FRET at individual hippocampal boutons

(A) *FR* (F^{Cit}/F^{Cer}) was reduced following acute application of 1 μM TTX (n = 11, $p < 0.001$).

(B) *Left:* APP-KK^{Cit} is not expressed at the membrane of HEK293 cells. *Right:* TTX had no effect on APP-KK^{Cer} – APP-KK^{Cit} E_m in hippocampal boutons (n =18 – 24, N = 4 - 5, $p > 0.7$).

(C) *FR* was increased following acute application of gabazine (GBZ, 30 μM, n = 10, $p < 0.001$).

(D) *FR* was increased by 100 Hz stimulation frequency (n = 12, $p < 0.05$).

(E) High frequency 100 Hz stimulation did not affect E_m in neurons pretreated by TeTx, while increased it by 2.5-fold in control cultures (n = 19 - 43, N = 4 - 6, $p < 0.05$).

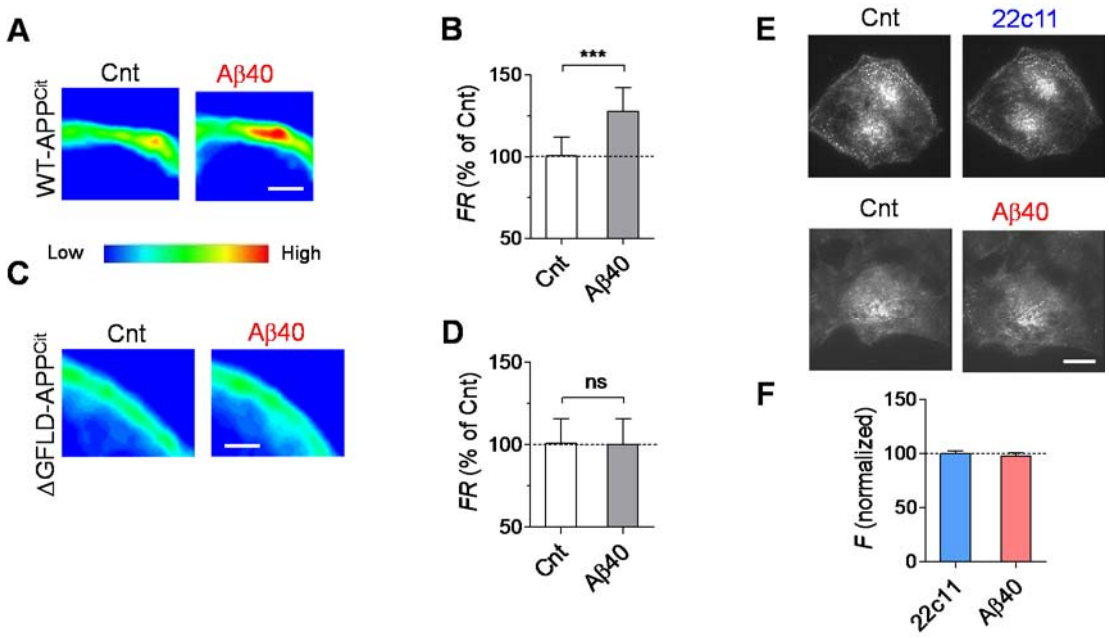

Figure S5, related to Figures 3 and 6. Effects of Aβ40 in heterologous expression systems

(A) Representative images displaying Cit fluorescence intensity exited by 440 nm laser before and 15 min after application of 100 nM Aβ40 in HEK293 transfected with WT-APP^{Cit} – WT-APP^{Cer}. (HEK cells were cultured in DMEM supplemented with fetal bovine serum (10%), L-glutamine (2 mM), penicillin (50 units/ml), streptomycin (50 μg/ml). All reagents were from Sigma. Cells were transiently transfected for 24 hours using Lipofectamine-2000 reagent according to the manufacturer recommendations, using modified growth medium without antibiotics. External solution was (mM): NaCl 137, KCl 5.4, $CaCl_2$ 1.2, $MgCl_2$ 1.2, HEPES 10, pH adjusted to 7.3). Imaging was done 36 – 48 h after transfection. Fluorescence intensities (arbitrary units) are coded using a pseudo color transformation. Scale bar: 2μM.

(B) Aβ40 increased WT-APP^{Cit} – WT-APP^{Cer} *FR* ($n = 47$, $p < 0.001$). Error bars represent ± s.e.m.

(C) Representative images displaying Cit fluorescence intensity exited by 440 nm laser before and 15 min after application of 100 nM Aβ40 in HEK293 transfected with ΔGFLD-APP^{Cit} – ΔGFLD-APP^{Cer}. Fluorescence intensities (arbitrary units) are coded using a pseudo color transformation. Scale bar: 2μM.

(D) Aβ40 did not affect ΔGFLD-APP^{Cit} – ΔGFLD-APP^{Cer} *FR* (n =28, p > 0.6). Error bars represent ± s.e.m.

(E) Representative TIRF images of COS-7 cells infected with APP^{mEGFP} before and after30 minutes incubation with 5 μg/ml 22c11 antibody (top images), and before and after 15 minutes incubation with 500 nM Aβ40 (bottom images). Scale bar: 10μM.

(F) Neither 22c11 (5 μg/ml: n = 60, p > 0.01), nor Aβ40 (500 nM: n = 20, p > 0.01) affected TIRF average fluorescence intensity of WT-APP^{Cit} compared to control.

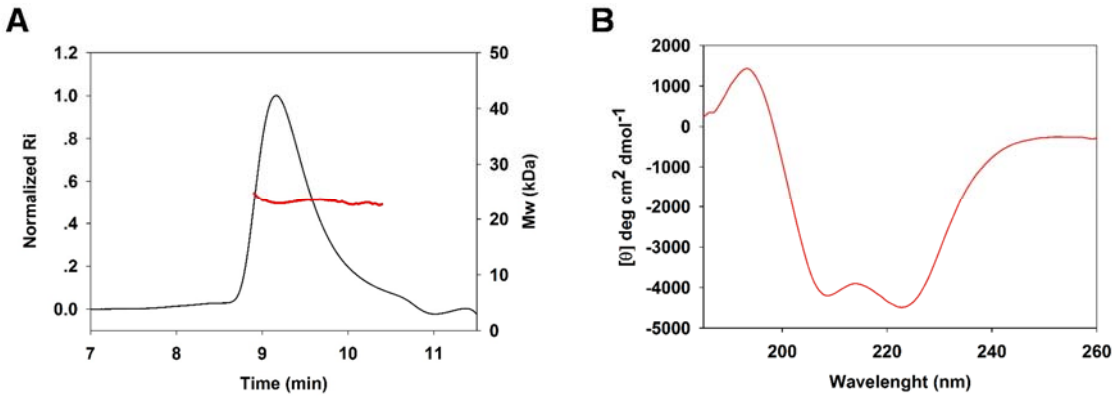

Figure S6, related to Figure 5A. Characterization of purified E1

(A) SEC-MALS measurement of E1 domain. A sample of E1 at 50 μM was measured at 25ºC, black line represents the elution profile of the sample (left Y axis). Red line represents the distribution of the sample population of the measurement by molecular weight (right Y axis).

(B) CD spectrum of the purified E1 domain of APP. 1 mg/ml of E1 was used to measure spectra at range of 180-260 resulted with distinct profile of α helix.

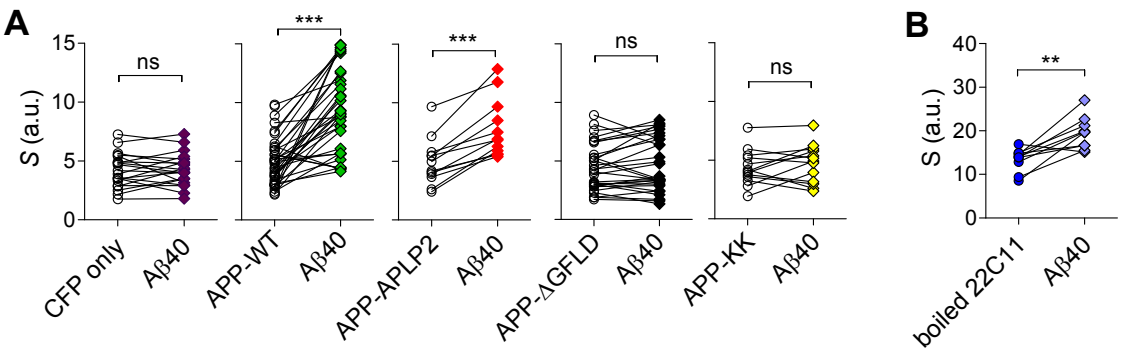

Figure S7, related to Figure 6. Identification of the APP molecular domain that is involved in Aβ40-mediated presynaptic enhancement

(A) Effects of 100 pM Aβ40 on the total presynaptic strength (*S*) per experiment in *APP*$^{-/-}$ hippocampal cultures transfected with different APP mutants.

(B) Pre-incubation with boiled 22c11 antibody (5 µg/ml, 2-3 hours) did not alter the effect of Aβ40 (100 pM) on presynaptic enhancement.

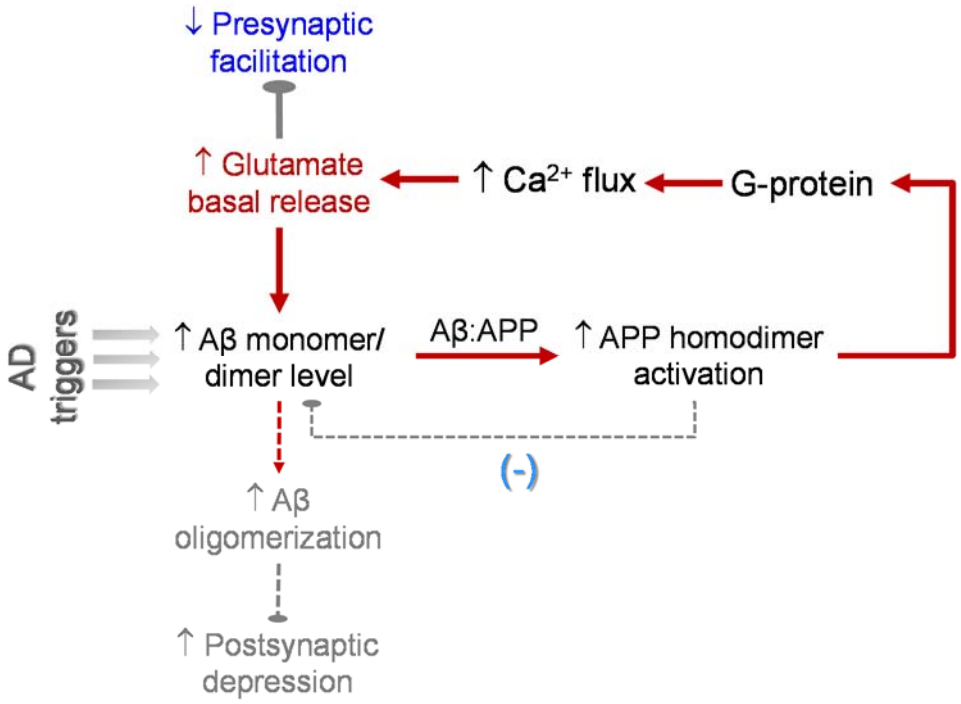

Figure S8. Proposed model of Aβ-mediated functions and dysfunctions at excitatory synapses. Under physiological conditions, a positive feedback loop between basal glutamate release and Aβ secretion may be compensated through a feedback inhibition of Aβ production, maintaining the basal extracellular glutamate and Aβ levels. Under pathological conditions, this negative feedback may be disrupted, resulting in hyperactivity of excitatory boutons and reduction in short-term synaptic facilitation. A remaining positive feedback between glutamate and Aβ release may lead to accumulation of the extracellular Aβ and subsequent Aβ oligomerization, resulting in postsynaptic depression and spine loss (Shankar et al., 2008).

Supplementary Methods:

Molecular biology. Wild type and mutants of human APP695 used for experiments in cultured neurons were constructed and expressed in pcDNA3.0 based vector under control of CMV promoter. To construct a wild type $hAPP_{695}$ fused to mCitrine and mCerulean cDNA, the mCitrine and mCerulean fluorescent genes were amplified with *Not*I and *Apa*I restriction site tagging primers and then subcloned into *Not*I and *Apa*I sites of plasmid pcDNA3-$hAPP_{695}$-YFP5 (Kaether et al., 2000) (kindly provided by Dr. Kaether).

In order to construct the APP-ΔGFLD mutants, where amino acids 22-128 are deleted, we first deleted the polylinker site from plasmid pcDNA3.0 by digestion with *Hin*dIII and *Eco*RV followed by blunting of *Hin*dIII site and re-ligation. Then we made use of *Kpn*I site that now is unique and cuts the APP gene just after amino acid 21. APP cDNA was amplified with primer 5'-GCTGGAGGTACCCGTTCCTGACAAGTGCA AATTC-3' introducing *Kpn*I site (underlined) and with primer 5'-GGACACGCTGAACTTGTGGCC-3' that anneals to amino acids 25-31 of any enhanced fluorescent protein. Then, the APP-ΔGFLD-mCitrine mutant was constructed by digestion of the PCR product with *Kpn*I and *Xho*I and ligation into the same sites of plasmid pcDNA3.0-$hAPP_{695}$-mCitrine. Subsequently, the APP-ΔGFLD-mCerulean mutant was constructed by subcloning of mCerulean cDNA into *Not*I and *Apa*I sites of plasmid pcDNA3.0-$hAPP_{695}$-ΔGFLD-mCitrine.

APP-APLP2-mCitrine chimera was engineered according to Shaked et al. (Shaked et al., 2006). In this mutant the amino acids 597-624 encompassing the Aβ domain of APP were substituted by a 44 amino acid region from mouse APLP2 immediately outside the predicted transmembrane domain (residues 616–659). The APP-APLP2 mutant was

constructed by ordering custom made plasmid containing 619-659 residues sequence of APLP2 digestion with *Pml*I and *Not*I sites and subcloned into *Pml*I and *Not*I sites that already exist on the APP-mCitrine gene.

APP-KK mutant was constructed by introducing KKQN (Maltese et al., 2001) before stop codon of APP-CFP/YFP using QuickChange PCR with complimentary primers 5'-GCATGGACGAGCTGTACAAGAAGAAGCAAAACTAAGGGCCCTATTCTATA GTGTCACC-3' and 5'-GGTGACACTATAGAATAGGGCCCTTAGTTTTGCTT CTTCTTGTACAGCT CGTCCATGC-3'. The integrity of constructs was confirmed by the sequencing analysis.

Transient cDNA transfections were performed using Lipofectamine-2000 reagents and neurons were typically imaged 18-24 h after transfection.

FRET imaging and analysis. Intensity-based FRET imaging was carried as described before (Laviv et al., 2010). For spectral analysis, mCerulean (Cer) was excited at 440 nm and fluorescence emission was measured between 400–600 nm, with a 10 nm λ step size. In order to reduce phototoxicity and photobleaching, most of the FRET experiments were performed using a narrowed emission spectrum (470–560 nm) composed of Cer peak (480 ± 10 nm) and a mCitrin (Cit) peak (530 ± 10 nm) containing Cit emission due to FRET, direct Cer excitation at 440 nm, and Cit emission tail. Cit was imaged at 515 nm (excitation) and 530–560 nm (emission). Photobleaching of Cit was carried out with 515 nm laser line, by a single point activation module for rapid and efficient multi-region bleaching. Images were acquired without averaging. Image acquisition parameters were optimized for maximal signal-to-noise ratio and minimal phototoxicity. Images were 512 × 512 pixels, with a pixel width of 92 – 110 nm. Z-stacks were collected from 3-4 μm optical slice, at 0.6 - 0.8μm steps.

Donor dequenching due to the desensitized acceptor was measured from Cer emission (460-500 nm) before and after the acceptor photobleaching. Mean FRET efficiency, E_m, was then calculated using the equation $E_m = 1 - I_{DA}/I_D$, where I_{DA} is the peak of donor emission in the presence of the acceptor and I_D is the peak after acceptor photobleaching. In order to exclude potential contribution of donor/acceptor ratio to FRET efficiency measurements, all FRET experiments were performed under saturation conditions of acceptor over donor. Detection of Cer and Cit signals was done using custom-written scripts in MATLAB as described earlier (Laviv et al., 2010). Briefly, regions of interest (ROIs) were marked at boutons that underwent Cit photobleaching. Average intensity of ROI was subtracted from background ROI intensity in close proximity to the bouton. All the boutons that exhibited Cit photobleaching by >90% of initial fluorescence intensity were included in the analysis. Non-bleached boutons at the same image area were analyzed to ensure lack of non-specific photobleaching due to image acquisition.

Single molecule fluorescence and bleaching step analysis in *Xenopus* oocytes: Single-molecule imaging on *X.Laevis* oocytes was performed after 18-24 hr expression at 18 degrees using TIRF microscopy set up as described elsewhere (Ulbrich and Isacoff, 2007). Briefly, oocytes were manually devitellinized and placed on high refractive index coverglass (n = 1.78) and imaged using Olympus 100X, NA 1.65 oil immersion objective at room temperature. EGFP tagged APP was excited using phoxX 488 (60mW) laser. A 495 nm long-pass dichroic mirror was used in combination with 525/50 nm band-pass filter for emission. 500-800 frames at the rate of 10 Hz were acquired for subunit counting using EMCCD (Andor iXon DV-897 BV). Only single, immobile and diffraction-limited spots were analyzed. The number of bleaching steps was determined manually for each single spot included in the analysis. 1000-1500 spots

from 5-10 oocytes from 3-5 different batches were analyzed for each construct. The error bars in subunit counting data show statistical uncertainty in counting and is given by √n, where n = number of counts.

Calcium imaging: Fluorescent calcium indicator Calcium Green 488 BAPTA-1 AM was dissolved in DMSO to yield a concentration of 1 mM. For cell loading, cultures were incubated at 37 °C for 30 min with 3 μM of this solution diluted in standard extracellular solution. Extracellular solution contained 20 μM DNQX to block recurrent activity and 50 μM APV to block calcium flux through NMDA receptors. Imaging was performed using FV1000 Olympus confocal microscope, under 488 nm (excitation) and 510 - 570 nm (emission), using 500 Hz line scanning. Ca^{2+} transients were quantified following averaging of 10 traces. Integral was calculated for $\Delta F/F$ per bouton before and after Aβ40 application. Integration time window was 600 ms, starting from the end of the stimulus.

Isolation of Aβ(1-40) monomer: Peptide was incubated at 1 mg/ml in denaturing buffer (50 mM Tris-HCl, pH 8.5 containing 7 M guanidine HCl and 5 mM EDTA) for ~14 h and monomer isolated using a Superdex 75 10/30 column eluted with 50 mM ammonium acetate, pH 8.5 (O'Nuallain et al. 2010). Aβ content was determined using ε_{275} = 1361 M^{-1} cm^{-1} (O'Malley & Walsh, unpublished) and peptide diluted to 50 μM with elution buffer. Aliquots were prepared on ice and stored at -80°C until used.

Oxidative cross-linking of Aβ(1-40)S26C and isolation of $[Aβ(1-40)S26C]_2$: Aβ(1-40)S26C monomer was isolated by SEC essentially as decribed above, then diluted to 40 μM, bubbled with oxygen (Airgas, Hingham, MA) and incubated at room temperature for 72 hours (O'Nuallain et al., 2010). Following cross-linking, the reaction mixture was frozen, lyophilised and dissolved at 1 mg/ml in denaturing buffer,

and dimer isolated from unreacted monomer and high molecular weight aggregates using a Superdex 75 16/60 column. Dimer content was determined using ε_{275} = 6244 M^{-1} cm^{-1} (O'Malley & Walsh, unpublished) and the concentration adjusted to 50 μM. Aliquots were prepared on ice and stored at -80ºC.

Cross-linking assay: Cross-linking assays were carried out according to the method described by Azem et al. (Azem et al., 1998). Reactions were carried out with 50 μM DSS in 10 mM Na-Hepes buffer (pH 7.4), 250 mM NaCl. Reactions were stopped after 1h by boiling the solution in SDS-loading buffer for 5 min. The samples were analyzed by SDS–PAGE with a 15% acrylamide gel and subjected to Western blotting with 6E10 antibody (Covance) followed by HRP-secondary antibody, according to standard procedures.

Aβ40-biotin binding assay: The assay was carried out according to the method described by Laeuren et al. (Lauren et al., 2009). Primary hippocampal culture from either WT or *APP*$^{-/-}$ mice were incubated in Tyrode solution (NaCl, 145mM; KCl, 3mM; glucose, 15mM; HEPES, 10mM; $MgCl_2$, 1.2mM; $CaCl_2$, 1.2mM; pH 7.4) with biotinilated Aβ40 (Anaspec) for 2 hr then fixed with 3.7% formaldehyde, washed three times with PBS, incubated in 65 °C for 2 hr, blocked for 20 min with 3% goat serum and 0.1% Triton X-100 in PBS, and incubated for 4 hr with alkaline-phosphatase-conjugated steptavidin in PBS supplemented with 1.5% goat serum and 0.05% Triton X-100. Finally, bound alkaline phosphatase was visualized by 5-bromo-4-chloro-3-indolyl phosphate/nitro blue tetrazolium reaction. Staining levels of neurons were visualized by Olympus FV300 with fixed illumination and exposure conditions and were quantified by comparing average staining intensity of neuron cell bodies difference from background for each condition.

Lentivirus vector construction and production. To obtain lentiviruses, cDNAs encoding APP^{mEGFP} and $APP^{mCherry}$ were cloned into lentiviral expression vector pLenti-CaMKIIa-hChR2-EYFP-WPRE (Yizhar et al., 2011). First, SwaI site was introduced into lentiviral expression vector by site-directed mutagenesis downstream of EYFP. APP^{mEGFP} and $APP^{mCherry}$ cDNA were amplified with forward 5'GCATGTACCGGTATGCTGCCCGGTTTGGCACTGC and reverse 5' GTAGTACAAATTTGTTACTTGTACAGCTCGTCCATG primers introducing AgeI and PmeI sites respectively. Digested PCR products were cloned into the lentiviral expression vector instead of AgeI-ChR2-EYFP-SwaI fragment.

Recombinant lentiviruses were produced as previously described (Pang et al., 2010). Briefly, HEK293 cells were transfected by calcium phosphate with four plasmids, the lentiviral shuttle vector, pLP/VSVG, pLP1 and pLP2. The HEK293 culture media was collected 24 and 48 h after transfection and filtered with 0.45 μm PVDF filter (Millipore) to remove cellular debris followed by centrifugation at 25,000 x RPM at 15^0C to concentrate the virus. Concentrated virus was dissolved in a small volume of PBS, aliquoted and stored frozen at -80°C.

***In Vivo* Injections.** *$APP^{-/-}$* and wild-type balb/c mice (6-8 weeks old) were used for stereotactic injection using standard procedures approved by the Tel Aviv University Animal Care Committee. Mice were immobilized on a Stoelting stereotactic apparatus under isoflurane anesthesia and small holes were made bilaterally in the skull at 2.2 mm posterior and 1.3 mm lateral to bregma for injection in the dentate gyrus region of the hippocampus. The needle of an Hamilton syringe filled with viral solution was lowered to a depth of 2 mm (from the dura) and the viral medium (1.2-1.5 μl of the mixture composed of 0.5 μl APP^{mEGFP} and 1 μl $APP^{mCherry}$ preparation) was injected using a microinjection pump (Harvard Apparatus) at a flow rate of 0.15 μl/min to each

hemisphere sequentially. Lentiviral vector titers were 10^8 to 10^9 per milliliter. The scalp was then sealed. All experiments were conducted 4-8 weeks after surgery.

Chemical reagents. FM4-64 (SynaptoRed C2), FM1-43 (SynaptoGreen C4) and Advasep-7 were purchased from Biotium; TTX, ω-conotoxin GVIA, and ω-agatoxin IVA from Alomone labs, thiorphan, TeTx and kynurenic acid from Sigma-Aldrich, BACE1 inhibitor IV, L-685,458 and rat Aβ1-40 from Calbiochem, biotinylated Aβ1-40 from AnaSpec, gabazine from Tocris. Human Aβ1-40 and Aβ1–40S26C were synthesized and purified by Dr. James I. Elliott at Yale University (New Haven, CT).

E1 expression and purification. The E1 domain (18-190 amino acids with a 6×Histidine tag at the C terminus) of APP was cloned into pET-28a vector using PCR for recombinant protein expression. The sequence was then verified by sequencing. The *E. coli* OrigamiB^{TM} (DE3) strain was used for protein expression in conjunction with the pET system. This strain carry the mutations in *trxB* and *gor* and is a *lac* permease (*lac*Y) deletion mutant, which allows uniform entry of IPTG into all cells of the population, producing a concentration-dependent, homogeneous level of induction. The mutations in *trxB* and *gor* are selectable on kanamycin and tetracycline, respectively. The protein was grown in YT×2 medium, containing 100 μg/ml ampicillin, 15 μg/ml kanamycin and 12.5 μg/ml tetracycline at 37˚C to an OD_{600} of 0.6. Expression was induced with 1 mM IPTG at 16˚ C. Cultures were harvested 40-48 hours after induction and stored at -80˚ C. Wild type E1 purification utilized metal-chelate chromatography, since the protein is tagged with a 8xHis-tag that has high affinity to Ni^{+2} beads. Cells were resuspended in Tris buffer (100 mM Tris pH=8, 500 mM NaCl) and 0.1% Triton X-100, DNase & protease inhibitor cocktail (sigma™) was added prior to lysis by microfluidizer. The lysate was then centrifuged for 1 hour at 14,000 rpm and the supernatant was loaded onto the Ni^{+2} chelate column. Proteins were eluted with Tris

buffer plus 300 mM imidazole. The collected fractions were diluted six fold with HEPES buffer without NaCl and then loaded onto a pre-equilibrated Heparin-Sepharose (Amersham Pharmacia) column. Fractions were eluted with a shallow linear gradient of buffer containing 50–1000 mM NaCl. Isolation of the E1 protein was completed with a final step using a Superdex-75 gel filtration column (Amersham Bioscience) with elution buffer containing 20 mM HEPES pH 7.4 and 150 mM NaCl. The purity of the protein was checked by SDS-PAGE gel electrophoresis. The protein was concentrated, flash frozen in liquid nitrogen and stored at -80˚C.

SEC-MALS*:* The absolute molecular masses of wild type E1 was obtain using multi-angle light scattering (MALS) using a HELEUS II (Wyatt Technology) photometer and a differential refractive index detector, Optilab T-rEX (Wyatt Technology, USA) connected to a KW 402.5-4f HPLC column (Shodex). The protein sample was eluted at 0.35 ml/min and detected at 280 nm. The SEC-MALS measurements were performed using PBS buffer pH=7.4, at 25°C. The protein was measured at 50 µM. Data analysis was performed with the ASTRA software package (Wyatt Technology, USA).

Circular dichroism*:* Recombinant E1 protein was evaluated by analyzing its secondary structure using CD spectroscopy. The measurement was performed using a Chirascan CD spectrometer (Applied Photophysics). Spectra were measured over the range of 260-180 nm at a scan rate of 1 nm/s. A cell with 0.1-mm path length was used. The spectrum is an average of five scans. The raw data were corrected by subtracting the contribution of the buffer to the signal. Then data were smoothed and converted to molar ellipticity units. Protein concentration was determined using the predicted extinction coefficient at 280 nm.

Analytical Size-exclusion Chromatography*:* The Aβ oligomeric state was determined by using HPLC system (Jasco) with an analytical Superdex 75 column (GE Healthcare). Monomeric and dimeric Aβ samples (50 μM) were loaded and eluted with 25 mM ammonium acetate, pH 8.5 at a flow rate of 0.5 ml/min. The peptides were detected by absorbance at 280 nm. Unbranched dextran standards (Sigma-Aldrich) with molecular masses of 5 kDa and 11.5 kDa were used for assessment of molecular weights of the tested Aβ40 species.

Immunocytochemistry: Cultures were fixed with 3.7% formaldehyde for 20 minutes than washed thoroughly with PBS, permeabilized with 0.25% Triton X-100 for 10 min, washed with PBS again and blocked for 1 hour with 10% goat serum. Primary antibodies, rabbit anti-APP (Y188) and guinea pig anti-synaptophysin1 (Syt1) were used to label APP and synapses overnight with 5% goat serum in 4 °C. Primary antibodies were visualized with fluorescent secondary antibodies, goat anti rabbit dylight 488 and goat anti guinea pig dylight 649. The mean fluorescent intensity of APP/Syt1 colocalized synapses was quantified.

TIRF imaging in COS-7 cells: TIRF was performed using COS-7 cell line. COS-7 cells were grown in DMEM supplemented with fetal bovine serum (10%), L-glutamine (2 mM), penicillin (50 units/ml), streptomycin (50 μg/ml). The cells were infected with APP^{Cit}. TIRF images were captured in growing medium in the incubation chamber (37^0C, 5% CO_2). The imaging setup consists of an iMIC inverted microscope with an oil-immersion plan-apochromatic 100X objective NA=1.45 (Olympus), polychrome V system (TILL photonics), 491 nm 100 mW DPSS laser "Calypso" (Cobolt), a polytrope condenser (iMIC Beam-switch for widefield, TIRF, FRAP illumination) and an ANDOR iXon DU 888D EMCCD camera (Andor, Belfast, Northern Ireland). The equipment is controlled by Live Acquisition Software (TILL photonics). Image

analysis was performed using custom-written scripts in MATLAB. Average intensity of regions of interest (ROIs) were marked and the background intensity from a close proximity to the ROI was subtracted. Same ROIs were compared before and after treatment.

Supplementary Reference

Azem, A., Weiss, C., and Goloubinoff, P. (1998). [22] Structural analysis of GroE chaperonin complexes using chemical cross-linking. In Methods in Enzymology, T.O.B. George H. Lorimer, ed. (Academic Press), pp. 253-268.

Kaether, C., Skehel, P., and Dotti, C.G. (2000). Axonal Membrane Proteins Are Transported in Distinct Carriers: A Two-Color Video Microscopy Study in Cultured Hippocampal Neurons. Mol Biol Cell *11*, 1213-1224.

Lauren, J., Gimbel, D.A., Nygaard, H.B., Gilbert, J.W., and Strittmatter, S.M. (2009). Cellular prion protein mediates impairment of synaptic plasticity by amyloid-beta oligomers. Nature *457*, 1128-1132.

Laviv, T., Riven, I., Dolev, I., Vertkin, I., Balana, B., Slesinger, P.A., and Slutsky, I. (2010). Basal GABA regulates GABA(B)R conformation and release probability at single hippocampal synapses. Neuron *67*, 253-267.

Maltese, W.A., Wilson, S., Tan, Y., Suomensaari, S., Sinha, S., Barbour, R., and McConlogue, L. (2001). Retention of the Alzheimer's amyloid precursor fragment C99 in the endoplasmic reticulum prevents formation of amyloid beta-peptide. J Biol Chem *276*, 20267-20279.

O'Nuallain, B., Freir, D.B., Nicoll, A.J., Risse, E., Ferguson, N., Herron, C.E., Collinge, J., and Walsh, D.M. (2010). Amyloid-beta-Protein Dimers Rapidly Form Stable Synaptotoxic Protofibrils. The Journal of Neuroscience *30*, 14411-14419.

Pang, Z.P., Cao, P., Xu, W., and Südhof, T.C. (2010). Calmodulin Controls Synaptic Strength via Presynaptic Activation of Calmodulin Kinase II. The Journal of Neuroscience *30*, 4132-4142.

Shaked, G.M., Kummer, M.P., Lu, D.C., Galvan, V., Bredesen, D.E., and Koo, E.H. (2006). Abeta induces cell death by direct interaction with its cognate extracellular domain on APP (APP 597-624). Faseb J *20*, 1254-1256.

Shankar, G.M., Li, S., Mehta, T.H., Garcia-Munoz, A., Shepardson, N.E., Smith, I., Brett, F.M., Farrell, M.A., Rowan, M.J., Lemere, C.A.*, et al.* (2008). Amyloid-beta protein dimers isolated directly from Alzheimer's brains impair synaptic plasticity and memory. Nat Med.

Ulbrich, M.H., and Isacoff, E.Y. (2007). Subunit counting in membrane-bound proteins. Nature methods *4*, 319-321.

Yizhar, O., Fenno, L.E., Prigge, M., Schneider, F., Davidson, T.J., O'Shea, D.J., Sohal, V.S., Goshen, I., Finkelstein, J., Paz, J.T.*, et al.* (2011). Neocortical excitation/inhibition balance in information processing and social dysfunction. Nature *477*, 171-178.